Pregnancy-Associated Plasma Protein-A2 (PAPP-A2): Tissue Expression and Biological Consequences of Gene Knockout in Mice

Cheryl A. Conover, Henning B. Boldt, Laurie K. Bale, Kari B. Clifton, Jacquelyn A. Grell, Jessica R. Mader, Emily J. Mason, and David R. Powell

The Endocrine Research Unit (C.A.C., H.B.B., L.K.B., K.B.C., J.A.G., J.R.M., E.J.M.), Division of Endocrinology, Metabolism, and Nutrition, College of Medicine Mayo Clinic, Rochester, Minnesota 55905; and Metabolism and Cardiology Research (D.R.P.), Lexicon Pharmaceuticals, Inc., The Woodlands, Texas 77381

Pregnancy-associated plasma protein-A2 (PAPP-A2) is a novel homolog of PAPP-A in the metzincin superfamily. However, compared with the accumulating data on PAPP-A, very little is known about PAPP-A2. In this study, we determined the tissue expression pattern of PAPP-A2 mRNA in wild-type (WT) mice and characterized the phenotype of mice with global PAPP-A2 deficiency. Tissues expressing PAPP-A2 in WT mice were more limited than those expressing PAPP-A. The highest PAPP-A2 mRNA expression was found in the placenta, with abundant expression in fetal, skeletal, and reproductive tissues. Heterozygous breeding produced the expected Mendelian distribution for the *pappa2* gene and viable homozygous PAPP-A2 knockout (KO) mice that were normal size at birth. The most striking phenotype of the PAPP-A2 KO mouse was postnatal growth retardation. Male and female PAPP-A2 KO mice had 10 and 25–30% lower body weight, respectively, than WT littermates. Adult femur and body length were also reduced in PAPP-A2 KO mice, but without significant effects on bone mineral density. PAPP-A2 KO mice were fertile, but with compromised fecundity. PAPP-A expression was not altered to compensate for the loss of PAPP-A2 expression, and proteolysis of PAPP-A2's primary substrate, IGF-binding protein-5, was not altered in fibroblasts from PAPP-A2 KO embryos. In conclusion, tissue expression patterns and biological consequences of gene KO indicate distinct physiological roles for PAPP-A2 and PAPP-A in mice. **(*Endocrinology* 152: 2837–2844, 2011)**

Pregnancy-associated plasma protein-A2 (PAPP-A2) is a novel metalloproteinase identified as a homolog of PAPP-A in the metzincin superfamily of pappalysins (1–4). Although PAPP-A was discovered as one of four proteins of placental origin found at high concentrations in plasma of pregnant women (5), there is now abundant evidence for functions of PAPP-A outside of pregnancy such as in skeletal growth and tissue response to injury (6–11). The physiological importance of PAPP-A2 is not known. Both enzymes have the potential to regulate the growth-promoting activities of IGF through their ability to cleave IGF-binding proteins (IGFBP) (reviewed in Ref. 6). However, there appear to be important differences in structure and function between the two that would likely result in distinct biological consequences.

PAPP-A2 shares 46% sequence identity with PAPP-A (3). However, unlike PAPP-A, PAPP-A2 is a noncovalently linked dimer of two 220-kDa subunits and is not able to bind to the surface of cells (12–17). PAPP-A2 exhibits robust proteolytic activity against IGFBP-5 and possibly also IGFBP-3 (3, 12). PAPP-A2 does not cleave IGFBP-4, the principal physiological substrate of PAPP-A (3, 6). Studies *in vitro* and *in vivo* indicate that cleavage of inhibitory IGFBP-4 by PAPP-A leads to enhanced IGF action (10, 11, 18, 19). On the other hand, PAPP-A deficiency results in compromised fetal growth and skeletal pheno-

ISSN Print 0013-7227 ISSN Online 1945-7170
Printed in U.S.A.

doi: 10.1210/en.2011-0036 Received January 12, 2011. Accepted April 27, 2011.
First Published Online May 17, 2011

Abbreviations: C_T, Cycle threshold; E16.5, embryonic d 16.5; ES, embryonic stem; IGFBP, IGF-binding protein; KO, knockout; MEF, mouse embryo fibroblasts; PAPP-A2, pregnancy-associated plasma protein-A2; pQCT, peripheral quantitative computed tomography; RPL19, ribosomal protein L19.

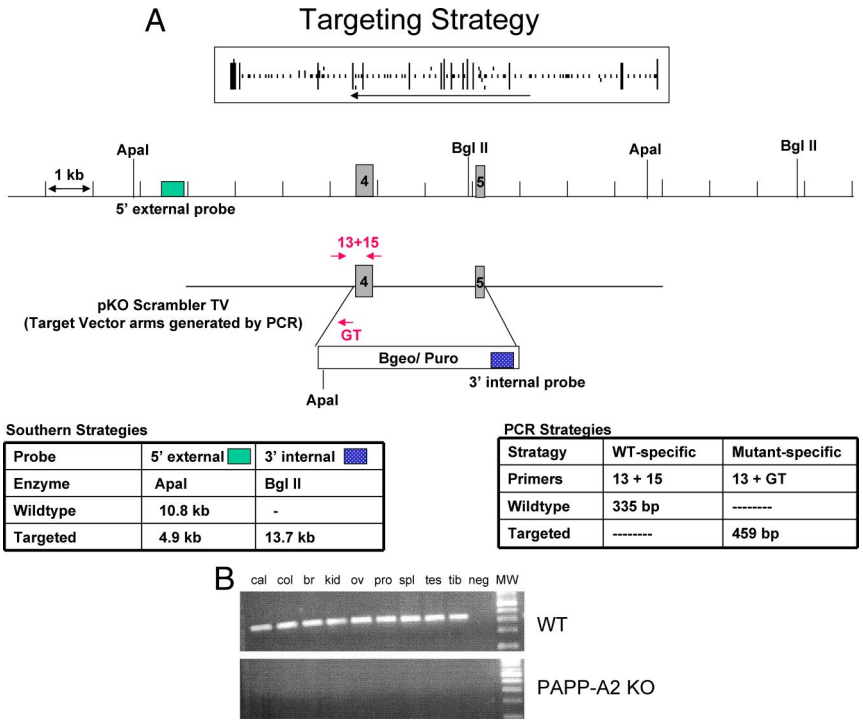

FIG. 1. Generation of PAPP-A2 KO mice. A, Schematic representation of targeting strategy described in *Materials and Methods* and PCR genotyping: 13, 5′-ACCCAATGACAGAGATTAGAG; 15, 5′-GGGATCATCACAGGATTCTC; GT, 5′-CCCTAGGAATGCTCGTCAAGA. B, PCR for PAPP-A2 expression in tissues from 8-wk-old WT mice (*top*) and PAPP-A2 KO mice (*bottom*) by endpoint PCR. cal, Calvaria; col, colon; br, brain; kid, kidney; ov, ovary; pro, prostate; spl, spleen; tes, testes; tib, tibia; neg, negative control; MW, molecular weight markers.

types (8, 20). The effect of IGFBP-5 proteolysis by PAPP-A2 is less clear, given that IGFBP-5 (and IGFBP-3) can inhibit or stimulate IGF action or have IGF-independent effects (21).

To gain insight into the physiological role of PAPP-A2 and its relationship to PAPP-A, this study was undertaken to determine the tissue expression pattern of PAPP-A2 compared with PAPP-A in wild-type (WT) mice and to characterize the phenotype of genetically modified mice deficient in PAPP-A2.

Materials and Methods

Generation of mutant PAPP-A2 mice

The PAPP-A2 targeting vector was derived using long-range PCR to generate the 5′ and 3′ arms of homology using C57BL/6J embryonic stem (ES) cell DNA as a template. The 3669-bp 5′ arm was generated using PAPP-A2 primers (5′-AGTCTTAGAGATGTGTAGTCGCTTGTCT-3′ and 5′-GTTGAGGACAACACCACCTGTAATGGAA-3′) and cloned using the TOPO cloning kit (Invitrogen, Carlsbad, CA). The 3826-bp 3′ arm was generated using PAPP-A2 primers (5′-GCAAAGGGTCTCTCATGGGAGCTAGAGG-3′ and 5′-GGGCACTCAGCACACAGAAGCAATGGTC-3′) and cloned using the TOPO cloning kit. The 5′ arm was excised from the holding plasmid using *Asc*I and *Sfi*I. The 3′ arm was excised from the holding plasmid using *Sfi*I and *Bgl*II. The arms were ligated to an *Sfi*I prepared selection cassette containing a β-galactosidase-neomycin fusion marker (Bgeo) along with a PGK promoter-driven puromycin-resistance marker and inserted into an *Asc*I/*Bgl*II cut pKO Scrambler vector (Stratagene, La Jolla, CA) to complete the PAPP-A2 targeting vector, which results in the deletion of coding exons 4–5. A schematic diagram of the vector and targeting strategy are shown in Fig. 1A.

The *Not*I linearized targeting vector was electroporated into C57BL/6J ES cells. G418/FIAU-resistant ES cell clones were isolated, and correctly targeted clones were identified and confirmed by Southern analysis using a 268-bp 5′ external probe, generated by PCR using PAPP-A2 primers (5′-CAAGTGAACTGCAAAGGTGC-3′ and 5′-GTTCTGCATCCTGCATTCTC-3′) and a 609-bp 3′ internal probe, amplified by PCR using Neo primers (5′-CCTCAGAAGAACTCGTCAAG-3′ and 5′-GGCAGCGCGGCTATCGTG-3′). Southern analysis using the 5′ external probe detected a 10.8-kb WT band and 4.9-kb mutant band in *Apa*I-digested genomic DNA, whereas the 3′ internal probe detected a 13.7-kb mutant band in *Bgl*II-digested genomic DNA. Six targeted ES cell clones were microinjected into C57BL/6 (albino) blastocysts to generate chimeric animals that were bred to C57BL/6 (albino) females, and the resulting heterozygous offspring were interbred to produce homozygous PAPP-A2-deficient mice and WT littermates. All studies performed on these mice were approved by Mayo Clinic's Institutional Animal Care and Use Committee.

RNA isolation

Tissue samples were freshly dissected, immediately placed in TRIzol reagent (Invitrogen), homogenized, and sheared through 21- and 23-gauge needles. Tissue homogenate was centrifuged to remove excess debris, and 0.2 ml chloroform per 1 ml TRIzol was added. Tubes were shaken vigorously for 45 sec, incubated at room temperature for 5 min, and centrifuged at 12,000 rpm at 4 C for 15 min. A second chloroform extraction was repeated for tissues with high protein or lipid content, and 0.5 ml isopropanol per 1 ml TRIzol was added to the aqueous phase. Smaller tissues such as ovary and prostate also had 6 μl glycogen (Invitrogen) added as a molecular carrier. Samples were incubated at room temperature for 15 min and then centrifuged at 10,000 rpm at 4 C for 10 min. The RNA pellet was washed twice with 75% ethanol, allowed to air dry, and resuspended in 10 μl molecular-grade water (Cellgro, Manassas, VA). To avoid contamination of genomic DNA, RNA was treated with deoxyribonuclease according to manufacturer's instructions (QIAGEN, Valencia, CA). Quantification and analysis of isolated RNA was performed using a NanoDrop Spectrophotometer (Wilmington, DE).

Real-time PCR

cDNA was reverse transcribed from RNA (1 μg) using TaqMan reverse transcription reagents (Applied Biosystems, Branchburg, NJ). Real-time RT-PCR of 25 μl were set up using iQ SYBR Green Supermix (Bio-Rad Laboratories, Hercules, CA).

The primer pairs were designed to distinguish between mouse PAPP-A and PAPP-A2 mRNA by positioning primer sequences in regions of low cDNA sequence similarity using OLIGO Primer Analysis Software (Molecular Biology Insights, Inc., Cascade, CO). The specificity of the primer pairs was verified by real-time PCR using two sets of specific primer pairs for each target gene and a range of cDNA templates derived from murine tissues and cell lines, resulting in very similar amplification from primer sets specific for the same target gene across all templates. The following primer sets were used: RPL19, forward 5′-CAATGCCAACTCCCGTCAGC-3′ and reverse 5′-TCTTGGATTCCCGGTATCTC-3′; PAPPA, forward 5′-GCCGTGGGAGCAATATC-3′and reverse 5′-ATGGACTCGCTGTTATGGTC-3′; and PAPPA2, forward 5′-GGTCACATGGAGTGCGCTAT-3′ and reverse 5′-CCGGTGGGACACACGAGATG-3′.

PCR was carried out using a Bio-Rad iCycler iQ5 multicolor real-time PCR detection system with samples tested in duplicate on 96-well plates. Amplicons (<300 bp) were generated in a two-step PCR (95 C for 10 sec, 60 C for 30 sec for 40 cycles) followed by melting curve analysis to exclude contamination of nonspecific products. Mouse ribosomal protein L19 (RPL19) was used as reference gene for all tissues analyzed (22). RPL19 expression was stable and abundant across all tissues and mouse genotypes [5 million copies per microgram RNA; cycle threshold (C_T) of ~17.5]. Normalization was performed by comparing C_T values of RPL19 expression within each tissue dataset, but not across different tissue datasets to avoid inappropriate normalization-derived inflation of expression data. Controls without template were included for each reaction plate. Absolute expression levels of target genes were determined by including dilution series of known amplicon concentrations on each real-time PCR plate to establish standard curves followed by conversion to copy number per microgram RNA by accounting for cDNA dilutions. Samples with amplification of target genes resulting in copy numbers below 200 in absolute expression levels, corresponding to C_T values of approximately 32, were considered to be the limit of detectable mRNA.

Skeletal and fat mass evaluations

Embryonic d 16.5 (E16.5) embryos were eviscerated, skinned, fixed in ethanol, and then stained with Alcian Blue 8GS (cartilaginous elements) and Alizarin Red S (mineralized elements) at 37 C for 3–5 d, as described previously (20). The stained skeletons were stored in 100% glycerol. Images were captured using a Nikon SMZ8000 microscope, DXM1200F digital camera, and ACT-1 software (Nikon, Tokyo, Japan). PCR-based sexing of mouse embryos was performed according to the method of McClive and Sinclair (23).

Peripheral quantitative computed tomography (pQCT) of the midshaft and distal metaphysis of the right femur was performed using a Stratec XCT Research SA Plus scanner with version 5.40 software (Norland Medical Systems, Fort Atkinson, WI), as described previously (8). Fat mass was analyzed using a PIXImus small animal densitometer (Lunar, Madison, WI).

Fertility

To assess effects of PAPP-A2 knockout (KO) on fertility, we bred female PAPP-A2 KO with male WT mice, male PAPP-A2 KO with female WT mice, KO × KO mice, and WT × WT mice (5 cages for each) starting at 8 wk of age. Time to first litter, time between litters, number of litters, and number of pups per litter were monitored for 4 months. Pups remained in the cage until d 19 to foster normal maternal instincts.

Primary cell cultures

Primary cultures of mouse embryo fibroblasts (MEF) were derived from E13.5 embryos. Embryos were washed, minced, and trypsinized, and single-cell suspensions were plated in high-glucose DMEM containing glutamine, penicillin, streptomycin, β-mercaptoethanol, and 10% fetal calf serum. Cells at passage 2 were used for experiments.

IGFBP protease activity

Primary cultures of MEF were washed and changed to serum-free medium. After 24 h, conditioned medium was collected for cell-free assay. IGFBP-3, IGFBP-4, and IGFBP-5 proteolysis was assayed as described previously (20), by incubating MEF-conditioned medium samples at 37 C for 6 h with ^{125}I-labeled IGFBP. Proteins were separated by SDS-PAGE and visualized by autoradiography.

TABLE 1. Gene expression: tissue distribution in WT mice

Tissue (n)	mRNA (copy number/μg RNA)	
	PAPP-A2	PAPP-A
Placenta (8)	1623614 ± 525354	6258 ± 1201[a]
Fetal head (20)	24448 ± 6259	19136 ± 1977
Fetal body (20)	17557 ± 5318	10448 ± 1705
Calvaria (7)	41542 ± 601	41500 ± 601
Prostate (5)	33755 ± 6365	9509 ± 1609[a]
Colon (6)	14447 ± 3095	10810 ± 757
Lung (7)	7626 ± 1282	1328 ± 162[a]
Ovaries (6)	5871 ± 2367	36828 ± 8494[a]
Tibia (9)	4679 ± 1324	61008 ± 3243[a]
Brain (7)	4599 ± 695	11161 ± 58[a]
Spinal cord (7)	2819 ± 768	31483 ± 5407[a]
Testes (5)	2418 ± 286	71578 ± 7135[a]
Kidney (5)	1621 ± 468	29816 ± 6611[a]
Spleen (6)	ND	10031 ± 719[a]
Soleus (9)	ND	1770 ± 338[a]
Mesenteric adipose tissue (5)	ND	27729 ± 9982[a]
Thymus (4)	ND	976 ± 154[a]
Uterus (6)	ND	24717 ± 7145[a]
Lymph nodes (5)	ND	7442 ± 1944[a]
Liver (6)	ND	604 ± 159
Subcutaneous adipose tissue (6)	ND	13801 ± 2311[a]
Skin (6)	ND	ND
Quadriceps muscle (6)	ND	11562 ± 2332[a]
Heart (6)	ND	36266 ± 6881[a]

Fetal and placental tissues were obtained at E18.5 from four pregnant WT mice. Other tissue harvests were from 8-wk-old mice. Results are mean ± SEM. ND, Not detectable (see *Materials and Methods*).

[a] $P < 0.05$, PAPP-A2 *vs.* PAPP-A.

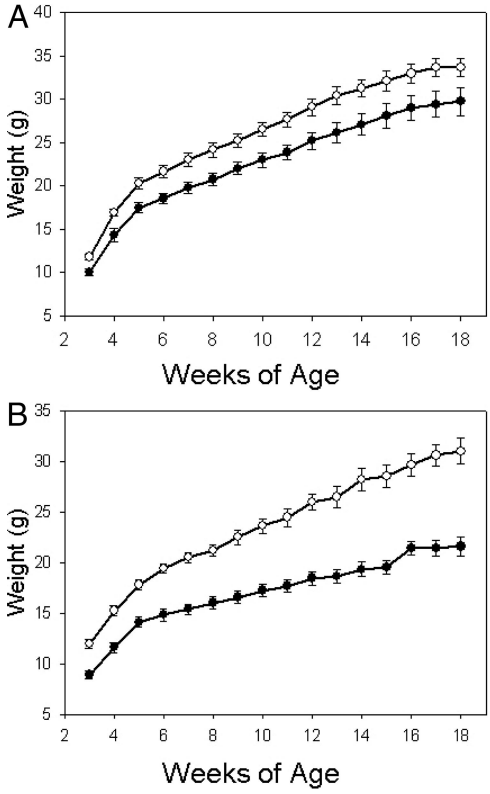

FIG. 2. Growth curves of WT (○) and PAPP-A2 KO (●) males (A) and females (B). Values are mean ± SEM of seven to nine individual weights.

Statistical analysis

Data are presented as mean ± SEM. Two-tailed unpaired *t* tests (JMP version 8.0 software; SAS Institute Inc., Cary, NC) were used to compare WT and PAPP-A2 KO groups. Two-tailed one-sample paired *t* tests on differences were used to compare PAPP-A and PAPP-A2 expression. $P < 0.05$ was considered statistically significant.

Results

PAPP-A2 expression in WT mice

Table 1 presents the expression data for PAPP-A2 in various tissues of WT mice. PAPP-A2 expression was highest in placenta, consistent with findings of Wang *et al.* (24), with mRNA levels 60-fold greater than in fetal tissue. The highest expression of PAPP-A2 in the adult was found in calvaria and prostate. PAPP-A2 expression was also detected in colon, lung, ovary, tibia, brain, spinal cord, testis, and kidney. No PAPP-A2 expression was found in spleen, skeletal muscle, adipose tissue, thymus, uterus, lymph nodes, liver, skin, and heart. PAPP-A expression levels in the same tissues are presented for relative comparison. The highest PAPP-A expression was seen in testis, bone, kidney, ovary, uterus, heart, and adipose tissue. All tissues examined, except for skin, had detectable PAPP-A mRNA levels, including placenta. However, mouse placenta expresses much lower levels of PAPP-A than human placenta (25).

Viability and growth of PAPP-A2 KO mice

Interbreeding of heterozygous mice gave rise to the expected Mendelian distribution for the *pappa2* gene. The male to female ratio for homozygous mutants was approximately 50:50. RNA prepared from tissues of 8-wk-old animals verified the complete loss of *pappa2* expression in homozygous mutants (Fig. 1B). Homozygous PAPP-A2 KO mice were viable, and male PAPP-A2 KO mice had approximately 10% lower body weight than male WT mice from 3–18 wk of age (Fig. 2A). The weight reduction in female PAPP-A2 KO mice was more pronounced than in males with an approximately 25% reduction over the first 3 wk after weaning, which then rose to 30% (Fig. 2B).

Male and female PAPP-A2 KO mice showed different patterns of body scaling. Males, although 10% smaller by weight on average, had overlapping weight ranges and were not significantly different. Similarly, body length was modestly smaller, but not significantly different. Measures of various major organs indicated a slight increase in the wet weight of most organs relative to body weight in PAPP-A2 KO *vs.* WT mice, but the increase was significant only for liver (Table 2). In contrast to the males, female

TABLE 2. Allometric measurements of 4-month-old PAPP-A2 KO and WT mice

	WT	PAPP-A2 KO
Males		
Body weight (g)	33.8 ± 1.22	30.2 ± 1.90
Heart[a]	0.43 ± 0.019	0.45 ± 0.014
Spleen[a]	0.24 ± 0.019	0.31 ± 0.019
Liver[a]	4.29 ± 0.566	4.79 ± 0.945[d]
Kidney[a]	0.53 ± 0.022	0.58 ± 0.023
Brain[a]	1.43 ± 0.054	1.43 ± 0.105
Testes[a]	0.35 ± 0.029	0.40 ± 0.022
Body length[b] (cm)	9.6 ± 0.09	9.2 ± 0.18
Femur length[c] (%)	16.2 ± 0.21	16.4 ± 0.45
Females		
Body weight (g)	31.3 ± 1.30	21.8 ± 1.05[d]
Heart[a]	0.39 ± 0.018	0.45 ± 0.019[d]
Spleen[a]	0.33 ± 0.018	0.41 ± 0.022[d]
Liver[a]	4.09 ± 0.200	4.75 ± 0.125[d]
Kidney[a]	0.47 ± 0.038	0.58 ± 0.023[d]
Brain[a]	1.58 ± 0.092	1.93 ± 0.087[d]
Ovaries[a]	0.046 ± 0.004	0.056 ± 0.005
Body length[b] (cm)	9.6 ± 0.14	8.6 ± 0.16[d]
Femur length[c] (%)	16.9 ± 0.37	17.8 ± 0.51

Results are mean ± SEM; n = 9 WT males, 9 PAPP-A2 KO males, 10 WT females, and 7 PAPP-A2 KO females.

[a] Organ weights expressed as a percentage of total body weight.

[b] Nose to anus.

[c] Femur length expressed as a percentage of total body length.

[d] $P < 0.05$, WT *vs.* PAPP-A2 KO.

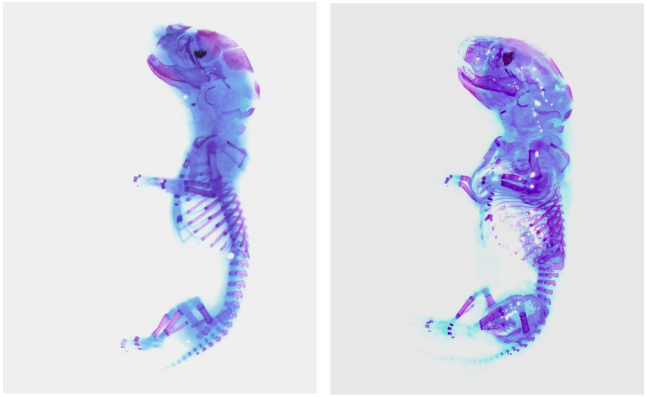

FIG. 3. Fetal development of PAPP-A2 KO mice. E16.5 embryos were stained with Alcian Blue 8GS (cartilaginous elements) and Alizarin Red S (mineralized elements), as described in *Materials and Methods*.

PAPP-A2 KO mice had significantly lower body weight and length compared with WT. Additionally, all organs except ovaries were disproportionally larger in the KO. Knockout of PAPP-A2 decreases overall body size, as measured by weight and length, to a greater degree than organ size; *i.e.* the soft organs are oversized in the KO relative to WT. Because the males are not significantly different in the indicators of body size, this difference is not significant. However, in the females, organ size is positively allometric relative to body size.

PAPP-A2 and the skeleton

Given the postnatal growth and skeletal phenotype of PAPP-A2 KO mice, we further investigated the effect of *pappa2* deficiency on skeletal development. Staining of E16.5 embryos indicated similar embryo lengths and no apparent developmental delay in mineralization of facial and cranial bones, vertebrae, and digits. Nine sex-matched littermate pairs of WT and PAPP-A2 KO embryos were evaluated, and a representative match is presented in Fig. 3.

There was no difference in cortical thickness of the femur between 4-month-old WT and PAPP-A2 KO mice as measured by pQCT (Table 3). Furthermore, proportional decreases in area and bone mineral content in midshaft (primarily cortical bone) and distal femur (primarily trabecular bone) resulted in no significant difference in bone mineral density in PAPP-A2 KO compared with WT bone. Body composition measured by dual-energy x-ray absorptiometry did not show any significant differences in percent fat mass between 4-month-old WT and PAPP-A2 KO mice, although there was a trend toward a decrease in percent fat mass in female PAPP-A KO compared with WT mice [22.9 ± 1.4% (n = 13) *vs.* 27.9 ± 2.5% (n = 12); $P = 0.09$]. Thus, the PAPP-A2 KO skeleton appears smaller but of similar composition.

PAPP-A2 and reproduction

Because PAPP-A2 is highly expressed in the placenta, we anticipated a reproductive phenotype in the PAPP-A2 KO mouse. Four breeding combinations of WT and PAPP-A KO mice were made (male/female): WT/WT, KO/KO, WT/KO, KO/WT. Matings were started at 8 wk of age and monitored for time to first litter, time between litters, number of litters over a period of 4 months, and number of pups per litter. Pups remained in the cage until d 19. Results are presented in Table 4. For the KO/KO compared with WT/WT matings, there was a delay to first litter (23.8 *vs.* 20.8 d), increased number of days between litters (26.3 *vs.* 22.0 d), and decrease in number of pups per litter (7.1 *vs.* 9.2). Interestingly, the mixed (male/female) KO/WT also showed an increased number of days to first litter (23.4 d) and between litters (25.1 d). On the other hand, the reproductive phenotype of WT males bred to PAPP-A2 KO females was similar to WT/WT matings. There was no significant difference in 19-d-old pup weights from WT/WT and KO/KO matings (8.8 ± 0.17 and 8.6 ± 0.17 g, respectively). Thus, PAPP-A2 KO mice

TABLE 3. Bone phenotype of 4-month-old PAPP-A2 KO and WT mice

	Male			Female		
	WT (n = 7)	KO (n = 8)	*P* value	WT (n = 10)	KO (n = 7)	*P* value
Midshaft						
Cort th (mm)	0.27 ± 0.01	0.27 ± 0.01	1.00	0.30 ± 0.01	0.29 ± 0.01	0.50
Area (mm^2)	2.3 ± 0.09	2.0 ± 0.09	0.03	2.6 ± 0.22	2.0 ± 0.12	0.03
BMC (mg; per 1-mm slice)	1.6 ± 0.06	1.5 ± 0.07	0.18	1.8 ± 0.12	1.4 ± 0.06	0.01
BMD (mg/cm^3)	699 ± 10	724 ± 9	0.09	693 ± 7	718 ± 16	0.32
Distal						
Area (mm^2)	4.0 ± 0.14	3.7 ± 0.14	0.09	4.4 ± 0.21	3.3 ± 0.12	<0.01
BMC (mg; per 1-mm slice)	2.0 ± 0.09	1.8 ± 0.08	0.13	2.3 ± 0.11	1.75 ± 0.05	<0.01
BMD (mg/cm^3)	499 ± 10	502 ± 14	0.87	527 ± 10	530 ± 10	0.82

pQCT of the midshaft and distal metaphysis of femurs was performed. Results are mean ± SEM. BMC, Bone mineral content; BMD, bone mineral density (mg/cm^3); Cort th, cortical thickness.

TABLE 4. Reproductive phenotype

	Male/female			
	WT/WT	KO/KO	WT/KO	KO/WT
Days from mating to first litter	20.8	23.8	21.6	23.4
Days between litters	22.0	26.3	22.4	25.1
Number of litters	19	20	23	19
Number of pups born	174	142	183	148
Pups/litter	9.2	7.1	8.0	7.8

WT and PAPP-A2 KO matings were monitored for 4 months; n = 5 pairs per breeding.

are fertile and produce viable offspring, although fecundity appears suboptimal.

IGFBP proteolysis

Primary MEF derived from E13.5 WT and PAPP-A2 KO mice were cultured and the conditioned media assayed for IGFBP-3, -4, and -5 protease activity. Conditioned media from WT and PAPP-A2 KO MEF showed similar activities, *i.e.* no IGFBP-3 proteolysis (data not shown) and equivalent IGFBP-4 and IGFBP-5 proteolysis (Fig. 4, A and B). Similar results were seen with MEF from male and female embryos (data not shown). Because PAPP-A has also been reported to cleave IGFBP-5 (26), PAPP-A mRNA expression was evaluated in MEF to determine whether there was up-regulation of PAPP-A to compensate for the loss of PAPP-A2 expression. However, there was no change in PAPP-A mRNA expression in PAPP-A2 KO MEF (Fig. 4C). Also, there was no change in PAPP-A mRNA expression in the tissues isolated from PAPP-A2 KO mice, *i.e.* placenta, prostate, bone, ovaries, testes, colon, lung, and kidney (data not shown).

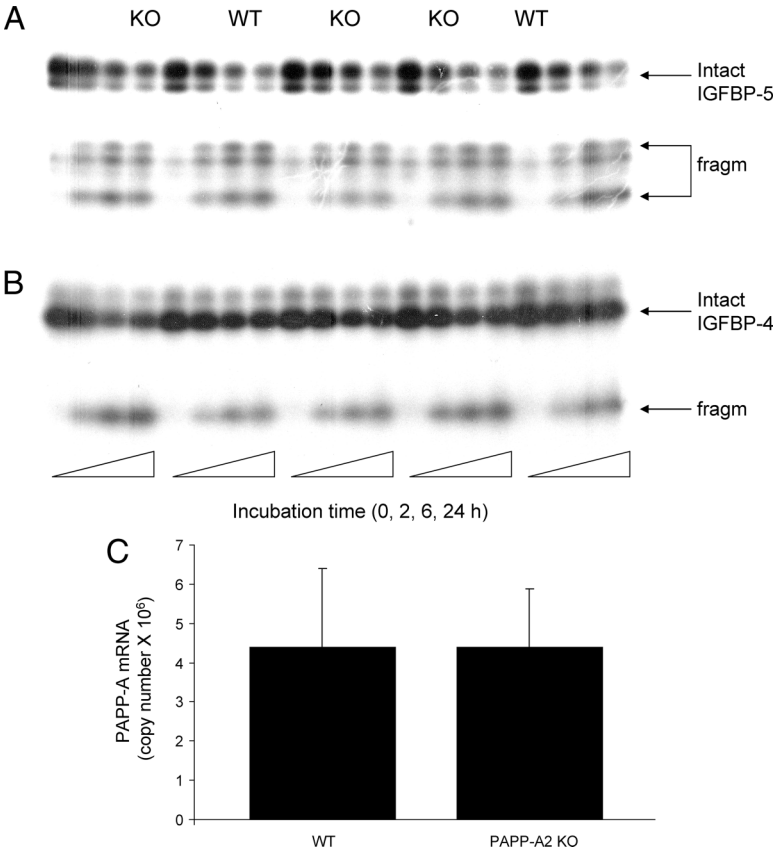

FIG. 4. A and B, Proteolysis of IGFBP-5 (A) and IGFBP-4 (B) in medium conditioned by embryonic fibroblasts derived from WT and PAPP-A2 KO mice, as described in *Materials and Methods*; C, PAPP-A mRNA expression in embryonic fibroblasts. Values are mean ± SEM of five experiments. fragm, Fragment.

Discussion

This study documents the differential expression of PAPP-A2 and PAPP-A in various fetal and adult mouse tissues and reports, for the first time, on the phenotype of PAPP-A2 KO mice.

Comparing the tissue patterns of relative expression, major differences between PAPP-A2 and PAPP-A expression were found in kidney, uterus, adipose tissues, heart, and placenta. PAPP-A is highly expressed in these tissues, whereas PAPP-A2 is moderately expressed in kidney and essentially not at all in uterus, adipose tissue, and heart. PAPP-A is expressed in mouse placenta, but at relatively low levels compared with PAPP-A2. These unique patterns of tissue expression support different physiological roles for PAPP-A2 and PAPP-A.

The highest PAPP-A2 expression was found in the placenta of WT mice, in concordance with a previous study by Wang *et al.* (24). In humans, expression of PAPP-A2 in placenta is up-regulated in hypertensive disorders of pregnancy, such as preeclampsia (27), and is one of several up-regulated genes in the placental molecular signature that distinguish the more severe hemolysis, elevated liver enzymes and low platelets (HELLP) syndrome from control and preeclampsia placenta (28). Although there are no data on the physiological function of PAPP-A2, it has been speculated that PAPP-A2 proteolysis of IGFBP-5 and release of IGF promotes fetoplacental growth (24, 27). PAPP-A2 has recently been identified as an IGFBP-5 protease in serum of pregnant women (29). Interestingly, PAPP-A is also highly expressed in human placenta, but maternal circulating PAPP-A levels are decreased in early pregnancy in disorders related to Down's syndrome and with increased risk of preeclampsia and low-birth-weight babies (30–32).

With the normally high levels of PAPP-A2 expression in placenta, prostate, ovary, and

testes, it was somewhat surprising that the PAPP-A2 KO mice were fertile, albeit with reduced fecundity. Importantly, this was not due to a compensatory increase in PAPP-A expression in MEF, placenta, or reproductive organs. Furthermore, proteolysis of IGFBP-5, the main IGFBP substrate for PAPP-A2, was not different in MEF from WT and PAPP-A2 KO embryos. This was not the case for MEF from PAPP-A KO embryos where no proteolysis of IGFBP-4, the main IGFBP substrate for PAPP-A, was found (20). These differential findings are likely due to the fact that PAPP-A is the only physiological IGFBP-4 protease, whereas several IGFBP-5 proteases have been described. One or more of these alternative proteases could help to normalize placental, developmental, and reproductive function regulated by IGFBP-5. Wagner and Christians (33) recently reported that a 2- to 3-fold difference in placental PAPP-A2 had no significant effect on placental mass, birth weight, or litter size and suggested redundancy with other IGFBP proteases, such as a disintegrin and metalloproteinase 12, which is highly expressed in placental tissue (34, 35). Interestingly, breeding pairs of male PAPP-A2 KO and female WT mice had increased number of days to first litter and days between litters. This did not occur with breeding pairs of female PAPP-A2 KO and male WT mice. This may indicate a novel role for the highly expressed PAPP-A2 in prostate physiology. Furthermore, the association of increased placental PAPP-A2 expression in preeclampsia (27) suggests a role for PAPP-A2 in pregnancy in addition to regulation of normal fetoplacental growth.

Also supporting a unique physiological role of PAPP-A2 was the finding that PAPP-A2 KO mice have reduced body weights compared with WT littermates. The lower body weights of the PAPP-A2 KO mice persisted over 4 months or even decreased further in females. The reason for the weight reduction of 25–30% for females compared with 10% for males observed in this study is unknown but may suggest important, but as yet unknown, interactions between PAPP-A2 and sex steroids. Unlike PAPP-A, significant body weight reductions occurred postnatally, not during early fetal development (20). PAPP-A2 was also highly expressed in adult bone, especially calvaria, likely affecting postnatal growth. This was of interest because Christians *et al.* (36) mapped a quantitative trait locus affecting body size in mice to a four-gene region including *pappa2* and found that this region also affected circulating levels of IGFBP-5. IGFBP-5 has been shown to promote IGF action during chondrocyte differentiation *in vivo* (37). Mohan *et al.* (38) mapped a quantitative trait locus affecting serum IGFBP-5 levels and bone mineral density to the same general region in a different cross of strains. There were no significant differences in bone mineral density in adult PAPP-A2 KO compared with WT mice in our study. These differential findings may be influenced by background genetics. We did not measure serum IGFBP-5 levels, because the available assays do not distinguish between intact and fragmented IGFBP-5.

In conclusion, studies reported herein are foundational in PAPP-A2 physiology. Further *in vitro* and *in vivo* study is necessary to better understand the regulation and action of PAPP-A2 in specific tissues.

Acknowledgments

Address all correspondence and requests for reprints to: Cheryl A. Conover, Ph.D., Mayo Clinic, 200 First Street SW, 5-194 Joseph, Rochester, Minnesota 55905. E-mail: Conover.Cheryl@mayo.edu.

These studies were funded in part by the Carlsberg Foundation (to H.B.B.).

Current address for H.B.B.: University of Aarhus, Department of Molecular Biology, DK-8000 Aarhus C, Denmark.

Disclosure Summary: D.R.P. is an employee of Lexicon Pharmaceuticals, Inc., and has received compensation in the form of salary and stock options.

References

1. **Farr M, Strübe J, Geppert HG, Kocourek A, Mahne M, Tschesche H** 2000 Pregnancy-associated plasma protein-E. Biochim Biophys Acta 1493:356–362
2. **Boldt HB, Overgaard MT, Laursen LS, Weyer K, Sottrup-Jensen L, Oxvig C** 2001 Mutational analysis of the proteolytic domain of pregnancy-associated plasma protein-A (PAPP-A): classification as a metzincin. Biochem J 358:359–367
3. **Overgaard MT, Boldt HB, Laursen LS, Sottrup-Jensen L, Conover CA, Oxvig C** 2001 Pregnancy-associated plasma protein-A2 (PAPP-A2), a novel insulin-like growth factor binding protein-5 proteinase. J Biol Chem 276:21849–21853
4. **Page NM, Butlin DJ, Lomthaisong K, Lowry PJ** 2001 The characterization of pregnancy associated plasma protein-E and the identification of an alternative splice variant. Placenta 22:681–687
5. **Lin TM, Galbert SP, Kiefer D, Spellacy WN, Gall S** 1974 Characterization of four human pregnancy-associated plasma proteins. Am J Obstet Gynecol 118:223–236
6. **Boldt HB, Conover CA** 2007 Pregnancy-associated plasma protein-A (PAPP-A): a local regulator of IGF bioavailability through cleavage of IGFBPs. Growth Horm IGF Res 17:10–18
7. **Harrington SC, Simari RD, Conover CA** 2007 Genetic deletion of pregnancy-associated plasma protein-A is associated with resistance to atherosclerotic lesion development in apolipoprotein E-deficient mice challenged with a high-fat diet. Circ Res 100:1696–1702
8. **Tanner SJ, Hefferan TE, Rosen CJ, Conover CA** 2008 Impact of pregnancy-associated plasma protein-A deletion on the adult murine skeleton. J Bone Miner Res 23:655–662
9. **Miller BS, Bronk JT, Nishiyama T, Yamagiwa H, Srivastava A, Bolander ME, Conover CA** 2007 Pregnancy associated plasma protein-A is necessary for expeditious fracture healing in mice. J Endocrinol 192:505–513
10. **Qin X, Wergedal JE, Rehage M, Tran K, Newton J, Lam P, Baylink DJ, Mohan S** 2006 Pregnancy-associated plasma protein-A in-

creases osteoblast proliferation *in vitro* and bone formation *in vivo*. Endocrinology 147:5653–5661
11. **Resch ZT, Simari RD, Conover CA** 2006 Targeted disruption of the pregnancy-associated plasma protein-A gene is associated with diminished smooth muscle cell response to insulin-like growth factor-I and resistance to neointimal hyperplasia after vascular injury. Endocrinology 147:5634–5640
12. **Boldt HB, Kjaer-Sorensen K, Overgaard MT, Weyer K, Poulsen CB, Sottrup-Jensen L, Conover CA, Giudice LC, Oxvig C** 2004 The Lin12-notch repeats of pregnancy-associated plasma protein-A bind calcium and determine its proteolytic specificity. J Biol Chem 279: 38525–38531
13. **Weyer K, Boldt HB, Poulsen CB, Kjaer-Sorensen K, Gyrup C, Oxvig C** 2007 A substrate specificity-determining unit of three Lin12-notch repeat modules is formed in trans within the pappalysin-1 dimer and requires a sequence stretch C-terminal to the third module. J Biol Chem 282:10988–10999
14. **Weyer K, Overgaard MT, Laursen LS, Nielsen CG, Schmitz A, Christiansen M, Sottrup-Jensen L, Giudice LC, Oxvig C** 2004 Cell surface adhesion of pregnancy-associated plasma protein-A is mediated by four clusters of basic residues located in its third and fourth CCP module. Eur J Biochem 271:1525–1535
15. **Sun IY, Overgaard MT, Oxvig C, Giudice LC** 2002 Pregnancy-associated plasma protein A proteolytic activity is associated with the human placental trophoblast cell membrane. J Clin Endocrinol Metab 87:5235–5240
16. **Conover CA, Harrington SC, Bale LK, Oxvig C** 2007 Surface association of pregnancy-associated plasma protein-A accounts for its colocalization with activated macrophages. Am J Physiol Heart Circ Physiol 292:H994–H1000
17. **Laursen LS, Overgaard MT, Weyer K, Boldt HB, Ebbesen P, Christiansen M, Sottrup-Jensen L, Giudice LC, Oxvig C** 2002 Cell surface targeting of pregnancy-associated plasma protein A proteolytic activity. J Biol Chem 277:47225–47234
18. **Ortiz CO, Chen BK, Bale LK, Overgaard MT, Oxvig C, Conover CA** 2003 Transforming growth factor-β regulation of the insulin-like growth factor binding protein-4 protease system in cultured human osteoblasts. J Bone Miner Res 18:1066–1072
19. **Byun D, Mohan S, Yoo M, Sexton C, Baylink DJ, Qin X** 2001 Pregnancy-associated plasma protein-A accounts for the insulin-like growth factor (IGF)-binding protein-4 (IGFBP-4) proteolytic activity in human pregnancy serum and enhances the mitogenic activity of IGF by degrading IGFBP-4 *in vitro*. J Clin Endocrinol Metab 86:847–854
20. **Conover CA, Bale LK, Overgaard MT, Johnstone EW, Laursen UH, Fuchtbauer E-M, Oxvig C, van Deursen J** 2004 Metalloproteinase pregnancy-associated plasma protein A is a critical growth regulatory factor during fetal development. Development 131:187–1194
21. **Schneider MR, Wolf E, Hoeflich A, Lahm H** 2002 IGF-binding protein-5: flexible player in the IGF system and effector on its own. J Endocrinol 172:423–440
22. **Chari R, Lonergan KM, Pikor LA, Coe BP, Zhu CQ, Chan TH, MacAulay CE, Tsao MS, Lam S, Ng RT, Lam WL** 2010 A sequence-based approach to identify reference genes for gene expression analysis. BMC Med Genomics 3:32
23. **McClive PJ, Sinclair AH** 2001 Rapid DNA extraction and PCR-sexing of mouse embryos. Mol Reprod Dev 60:225–226
24. **Wang J, Qiu Q, Haider M, Bell M, Gruslin A, Christians JK** 2009 Expression of pregnancy-associated plasma protein A2 during pregnancy in human and mouse. J Endocrinol 202:337–345
25. **Qin X, Sexton C, Byun D, Strong DD, Baylink DJ, Mohan S** 2002 Differential regulation of pregnancy associated plasma protein (PAPP)-A during pregnancy in human and mouse. Growth Horm IGF Res 12:359–366
26. **Rivera GM, Fortune JE** 2003 Selection of the dominant follicle and insulin-like growth factor (IGF)-binding proteins: evidence that pregnancy-associated plasma protein A contributes to proteolysis of IGF-binding protein 5 in bovine follicular fluid. Endocrinology 144: 437–446
27. **Nishizawa H, Pryor-Koishi K, Suzuki M, Kato T, Kogo H, Sekiya T, Kurahashi H, Udagawa Y** 2008 Increased levels of pregnancy-associated plasma protein-A2 in the serum of pre-eclamptic patients. Mol Hum Reprod 14:595–602
28. **Buimer M, Keijser R, Jebbink JM, Wehkamp D, van Kampen AH, Boer K, van der Post JA, Ris-Stalpers C** 2008 Seven placental transcripts characterize HELLP-syndrome. Placenta 29:444–453
29. **Yan X, Baxter RC, Firth SM** 2010 Involvement of pregnancy-associated plasma protein-A2 in insulin-like growth factor (IGF) binding protein-5 proteolysis during pregnancy: a potential mechanism for increasing IGF bioavailability. J Clin Endocrinol Metab 95: 1412–1420
30. **Wald NJ, Watt HC, Hackshaw AK** 1999 Integrated screening for Down's syndrome based on tests performed during the first and second trimesters. N Engl J Med 341:461–467
31. **Smith GC, Stenhouse EJ, Crossley JA, Aitken DA, Cameron AD, Connor JM** 2002 Early-pregnancy origins of low birth weight. Nature 417:916
32. **Smith GC, Stenhouse EJ, Crossley JA, Aitken DA, Cameron AD, Connor JM** 2002 Early pregnancy levels of pregnancy-associated plasma protein A and the risk of intrauterine growth restriction, premature birth, preeclampsia, and stillbirth. J Clin Endocrinol Metab 87:1762–1767
33. **Wagner PK, Christians JK** 2010 Altered placental expression of PAPPA2 does not affect birth weight in mice. Reprod Biol Endocrinol 8:90–97
34. **Gilpin BJ, Loechel F, Mattei MG, Engvall E, Albrechtsen R, Wewer UM** 1998 A novel, secreted form of human ADAM 12 (meltrin α) provokes myogenesis in vivo. J Biol Chem 273:157–166
35. **Loechel F, Fox JW, Murphy G, Albrechtsen R, Wewer UM** 2000 ADAM 12-S cleaves IGFBP-3 and IGFBP-5 and is inhibited by TIMP-3. Biochem Biophys Res Commun 278:511–515
36. **Christians JK, Hoeflich A, Keightley PD** 2006 PAPPA2, an enzyme that cleaves an insulin-like growth-factor-binding protein, is a candidate gene for a quantitative trait locus affecting body size in mice. Genetics 173:1547–1553
37. **Kiepe D, Ciarmatori S, Haarmann A, Tönshoff B** 2006 Differential expression of IGF system components in proliferating *vs.* differentiating growth plate chondrocytes: the functional role of IGFBP-5. Am J Physiol Endocrinol Metab 290:E363–E371
38. **Mohan S, Masinde G, Li X, Baylink DJ** 2003 Mapping quantitative trait loci that influence serum insulin-like growth factor binding protein-5 levels in F2 mice 9MRL/MpJ X SJL/J). Endocrinology 144:3491–3496